Determining erosion rates in Allchar (Macedonia) to revive the lorandite neutrino experiment

Pieter Vermeesch[1], *Martin Rittner*[1],
Irene Schimmelpfennig[2], *Lucilla Benedetti*[2], *ASTER Team*[2,3]

[1] London Geochronology Centre, Department of Earth Sciences, University College London, Gower Street, London WC1E 6BT, United Kingdom

[2]Aix-Marseille Université, CNRS, IRD, Coll. France, UM 34 CEREGE, Technopôle de l'Environnement Arbois-Méditerranée, BP 80, 13545 Aix-en-Provence, France.

[3]consortium: Georges Aumaître, Didier Bourlès and Karim Keddadouche

Keywords: cosmogenic nuclides, neutrinos, Macedonia

Abstract

^{205}Tl in the lorandite ($TiAsS_2$) mine of Allchar (Majdan, FYR Macedonia) is transformed to ^{205}Pb by cosmic ray reactions with muons and neutrinos. At depths of >300m, muogenic production would be sufficiently low for the 4.3 Ma old lorandite deposit to be used as a natural neutrino detector. Unfortunately, the Allchar deposit currently sits at a depth of only 120m below the surface, apparently making the lorandite experiment technically infeasible. We here present 25 erosion rates estimates for the Allchar area using in-situ produced cosmogenic ^{36}Cl in carbonates and ^{10}Be in alluvial quartz. The new measurements suggest long term erosion rates of 100-120 m/Ma in the silicate lithologies that are found at the higher elevations of the Majdanksa River valley, and 200-280 m/Ma in the underlying marbles and dolomites. These values indicate that the lorandite deposit has spent most of its existence at depths of >400m, sufficient for the neutrinogenic ^{205}Pb component to dominate the muon contribution. Our results suggest that this unique particle physics experiment is theoretically feasible and merits further development.

1 Introduction

When four hydrogen nuclei (protons) fuse to form one helium nucleus in the solar core, two of them convert to neutrons, releasing two neutrinos in the process. One of the definitive tests of this so-called Standard Solar Model is to measure the flux of those neutrinos. In order to detect these elusive particles, physicists have devised a number of experiments that broadly fall into two categories.

One group of experiments (Sudbury Neutrino Experiment, Super-Kamiokande, IceCube, Borexino) measures the light that is emitted when neutrinos scatter off electrons in water or a scintillation fluid. A second group (Homestake, Gallex, Sage) measures the radiation produced by neutrino reaction products such as Ar, Ge, and B (Bahcall et al., 1996). Because neutrino interactions are so rare, most of these experiments are massive in size and cost, with only one notable exception.

In 1976, Melvin Freedman proposed that the reaction ^{205}Tl (ν,e$^-$) ^{205}Pb could form the basis of a natural neutrino detector with the following advantages over alternative experimental designs (Freedman et al., 1976):

1. Thanks to the relatively large nuclear cross section of the reaction and the 16 Myr half life of ^{205}Pb, sufficient amounts of the reaction product can accumulate over geologic time to be measured by (Shottky) mass spectrometry on a sample of just a few kilograms of thallium-bearing minerals such as lorandite ($TlAsS_2$).

2. The resulting neutrino flux is a long term average over geologic time that may be more informative than the snapshot view of solar activity provided by artificial detectors.

3. Tl is sensitive to a wider range of neutrino energies than any other detector.

The world's largest accumulation of Tl-bearing minerals, and the only one suitable as a neutrino detector, is found in the Allchar mine in the former Yugoslavian republic of Macedonia. This deposit contains an estimated 500 tonnes of thallium, mostly in the form of lorandite with a geologic age of 4.3 Ma (Neubauer et al., 2009). In 1983, the international LOREX (LORandite EXperiment) collaboration was set up with the aim to investigate the feasibility of Freedman's idea (Pavićević, 1988). It was quickly realised that the Achilles heel of the proposal was the relatively shallow depth (120m) of the Allchar mine (Neumaier et al., 1991).

Besides neutrino reactions, a second production mechanism for ^{205}Pb is by cosmic ray muons. Whereas ^{205}Pb production by neutrinos is effectively independent of depth, the muon flux decreases exponentially with depth. But at 120m, the (fast) muon pathway still produces a significant background signal of ^{205}Pb. This paper shows that the burial depth of the lorandite may have been significantly greater in the past, because 4.3 million years worth of erosion may have removed a significant amount of overburden. The erosion rate, and hence the magnitude of the muogenic ^{205}Pb contribution, may be estimated by analysing other cosmogenic nuclides such as ^{36}Cl and ^{10}Be.

In 1991, the steady-state erosion rate of the Allchar area was estimated by a single ^{36}Cl measurement in limestone (Dockhorn et al., 1991). The ^{36}Cl concentration was found to be high, leading to the conclusion that erosion had been negligible, and that the lorandite had spent most of its 4.3 Ma lifetime at or near a depth of 120m. This conclusion all but terminated the geological neutrino detector and the physics community moved on to other experiments. This paper raises several issues with the Dockhorn et al. (1991) study, suggesting that the lorandite project may have been aborted prematurely (Section 2).

Pavićević et al. (2016) recently conducted a cosmogenic ^{36}Cl – ^{21}Ne – ^{26}Al study to re-evaluate the erosion rates in the Allchar area. They estimated erosion rates to fall in the 50-100 m/Ma range, which is much higher than the values obtained by Dockhorn et al. (1991). Unfortunately, the Pavićević et al. (2016) study

suffers from two methodological issues. First, it primarily focuses on the two lorandite-bearing mines (Crven Dol and Centralni Deo, Figure 1), which were considered to be the most relevant to the neutrino experiment. These sites also suffer from significant anthropogenic disturbance. This intrinsically leads to over-estimated erosion rates. Second, Pavićević et al. (2016) chose not to report any of their ^{10}Be results because "*the nominal erosion rates calculated on the basis of these ^{10}Be AMS measurements were considerably smaller than those obtained on the basis of ^{21}Ne, ^{26}Al, and ^{36}Cl concentrations*". We find this line of reasoning to be questionable, because ^{10}Be is generally considered to be the most reliable and least problematic cosmogenic nuclide.

To improve on these previous research efforts, we here present the results of a thorough cosmogenic nuclide investigation combining ^{36}Cl and ^{10}Be measurements in carbonates and quartz from bedrock samples and Majdanska River sediments (Sections 3-5). This two-pronged approach allows us to quantify the spatial variability of apparent erosion rates that may have affected previous erosion rate studies (Dockhorn et al., 1991; Pavićević et al., 2016), whilst simultaneously providing us with more robust catchment-wide erosion rate estimates (Section 6).

2 Previous erosion rate studies

Dockhorn et al. (1991) present the preliminary results of an uncompleted depth profile study. They report the ^{36}Cl/Cl ratio of a single sample of carbonate collected from 23m depth at an undisclosed location. No further compositional information is provided, although the total chlorine content of the sample is speculated to have been overestimated. At a depth of 23m, the poorly constrained muogenic production of ^{36}Cl far outweighs the much better constrained nucleogenic component. The lack of analytical detail and the suboptimal sampling strategy put into question the value of this erosion rate estimate. Furthermore, cosmogenic nuclide geochronology has greatly matured as a science since 1991.

A lot more is known now about the complex production systematics of ^{36}Cl in carbonates, including the effect of thermal neutron reactions on ^{35}Cl (Bierman et al., 1995; Stone et al., 1998; Alfimov and Ivy-Ochs, 2009; Schimmelpfennig et al., 2009), and the first order effect of sample preparation on the meteoric ^{36}Cl component (Merchel et al., 2008). These factors, if not accounted for, lead to an overestimation of the spallogenic ^{36}Cl content. Thus, the erosion rates of the Allchar area may have been greatly underestimated and ought to be re-evaluated using modern insights and methodologies.

In a recent study, Pavićević et al. (2016) presented a dataset of ^{26}Al (in quartz; 15 samples), ^{36}Cl (in carbonate; 3 samples), ^{3}He (in pyroxene; 1 sample), and ^{21}Ne (in quartz, sanidine or pyroxene; 8 samples). These samples were collected in bedrock directly above the two lorandite ore bodies (Crven Dol and Centralni Deo) in order to generate the most relevant erosion rate estimates for the lorandite neutrino project. Double-dating of hydrothermal vein quartz with ^{21}Ne and ^{26}Al yielded discordant erosion rate estimates, with an excess of stable ^{21}Ne relative to radioactive ^{26}Al. This discordance may be attributed to a complex exposure history, or simply to the presence of nucleogenic or magmatic ^{21}Ne in the samples. Unfortunately, no ^{10}Be measurements are reported that could distinguish between these two scenarios.

Pavićević et al. (2016) propose erosion rates of 50-100 m/Ma for the two lorandite localities, with individual estimates covering a huge range from 20-370 m/Ma. This range does not allow a clear-cut decision as to whether the long term erosion rate exceeds the 50 m/Ma cutoff required for the geological neutrino detector to be feasible. We address this problem with a different sampling strategy that combines bedrock samples and modern river sediments collected from the entire catchment area.

3 Sampling strategy

A two square kilometre area near the village of Majdan (41.157°N, 21.947°E) was combed out in search of suitable samples for cosmogenic nuclide analysis (Figure 1.a). The sampling strategy included four different kinds of sites:

1. The summits of the highest hills, which are covered by andesitic volcanics, and are expected to yield the lowest erosion rates.

2. Rare bedrock exposures in the canyons of tributaries to the Majdanska River that are carved out in dolomite and marble and are expected to yield the highest erosion rates.

3. Bedrock exposures on the steep slopes in between the above two settings, which consist of andesite, tuffs, marble and every conceivable reaction product of these end members.

4. Modern sand and gravel from the Majdanska River, which contain a wide range of lithologies including many quartz bearing phases (gneiss, granite). These are expected to yield intermediate erosion rates that are representative for the catchment-wide average of the area upstream of Majdan.

Unsurprisingly, we found that the vicinity of the lorandite ore bodies was severely affected by human activity. Thus, although these areas have the highest relevance to the proposed neutrino detector, they are the least well suited for cosmogenic nuclides studies as these require steady-state conditions. In contrast, the area between the Crven Dol and Centralni Deo sites has seen little anthropogenic disruption. We would argue that the apparent erosion rates from this area are more representative of the long term trends in the field area.

At each sampling location, the orientation of the sampled surface and the azimuth and elevation of the horizon were carefully measured, as these are needed to correct the ^{36}Cl and ^{10}Be concentrations for topographic shielding (Table 1). A total of 19 samples were collected, including 10 carbonates, 5 volcanic rocks, and 4 samples of modern river sediment (gravel and sand).

4 Methods

Upon their arrival in the UK, the hand specimens were cut into thick sections and their chemical and mineralogical composition were analysed by QEMSCAN (Quantitative Evaluation of Minerals by SCANning electron microscopy, Allen et al., 2012) at UCL. This reveals that the interplay between recent volcanic activity and the carbonate basement has produced a wide diversity of lithologies in the field area. The carbonate samples exhibit the full range of compositions from nearly pure dolomite to nearly pure calcite. Meanwhile, the volcanic samples feature sufficiently large and abundant phenocrysts for cosmogenic ^{36}Cl analysis. After completion of the QEMSCAN analyses, all the samples were shipped to CEREGE for cosmogenic nuclide analysis using ^{36}Cl (18 samples) and ^{10}Be (6 samples).

Carbonate and silicate samples were crushed and sieved to 250-500μm grain size. The magnetic fraction was removed from the silicate samples. Before any chemical treatment, whole rock sample splits were kept aside for analysis of the chemical composition by ICP-OES (major oxides) and ICP-MS (trace elements) at SARM-CRPG (Nancy, France). The samples were washed, and for the carbonates (silicates), 10 wt% (20 wt%) were etched of the grain surfaces by 2M HNO_3 (a mixture of concentrated HF and 2M HNO) and discarded. In case of the silicates, a 1 g split was taken from the resulting material for analysis of the major oxides (to know the concentrations of the target elements for ^{36}Cl production Ca, K, Ti and Fe) at SARM-CRPG. The carbonates and the remaining sample material of the silicates were dissolved after adding a spike enriched in ^{35}Cl.

In case of the carbonates, a split of this solution was taken for analyses of the target elements Ca and K by ICP-OES at CEREGE. $AgNO_3$ was added to precipitate AgCl, which was extracted and redissolved

with NH_3. $Ba(NO_3)_2$ was added to precipitate $BaSO_4$, which was filtered out and discarded. The pH was lowered and AgCl precipitated once more, which was extracted and dried for measurement at the ASTER Accelerator Mass Spectrometer (AMS) facility in CEREGE (Arnold et al., 2013).

Sediment samples were prepared similarly, but had the magnetic fraction removed in a Frantz separator first, before dissolving the carbonate fraction as described above. The undissolved silicate minerals were retained for Be measurement. Samples for ^{10}Be analysis were crushed, sieved and washed. The magnetic fraction was removed by Frantz magnetic separator. Carbonate was removed with HCl. The grains were then leached in a mixture of HCl and H_2SiF_6 . Atmospheric ^{10}Be was removed by etching 3 times ∼10 wt% off the surface of the remaining quartz grains with HF.

A ^{9}Be carrier was added to the residuum which was subsequently dissolved in hydrofluoric acid. HF was evaporated and the sample redissolved in HCl. Raising the pH by addition of NH_3 yielded $Be(OH)_2$ precipitate which was separated, dried, and redissolved with HCl. Fe and Mn were removed by ion exchange columns loaded with DOWEX 1×8 resin. Beryllium was recovered and $Be(OH)_2$ precipitated with NH_3 , separated, and dried again. The samples were redissolved in HCl, and loaded onto ion exchange columns of DOWEX 50W×8 resin. B was removed, and finally Be recovered, precipitated, centrifuged, redissolved in HNO_3 and finally dried down in porcelain crucibles. The samples were oxidised to BeO in a furnace at 700°C, before preparation for AMS analysis at ASTER (Arnold et al., 2010).

Erosions rates were inferred from the ^{36}Cl and ^{10}Be data using the spreadsheet of Schimmelpfennig et al. (2009) and CosmoCalc version 3.0 (Vermeesch, 2007). Production rates were determined using the scaling model of Stone (2000), assuming Sea Level and High Latitude (SLHL) spallation values of 42.2 at[^{36}Cl]/(g[Ca]·yr) for Ca (Schimmelpfennig et al., 2011), 148.1 at/(g·yr) for K (Schimmelpfennig et al., 2014), 13 at/(g·yr) for Ti (Fink et al., 2000), and 1.9 at/(g·yr) for Fe (Stone et al., 2005). Catchment-wide erosion rates for samples 11, 15, 17 and 20 were calculated using the average latitude and elevation obtained from a digital elevation model (von Blanckenburg, 2005), using only the area occupied by carbonates and quartz-bearing rocks for ^{36}Cl and ^{10}Be, respectively.

5 Results

The Allchar deposit is located in the catchment of the Majdanska River, which is underlain by Triassic dolomite, and andesitic lavas and rhyolitic tuffs of Pliocene age (Figure 1.b). The dolomite has undergone various degrees of contact metamorphism and hydrothermal alteration. This is reflected in the chemical and mineralogical composition, as determined by QEMSCAN and ICP-OES/MS (Table 2). Carbonate rocks range from the original dolomite to completely recrystallised marbles made of pure calcite. ^{35}Cl concentrations follow a bimodal distribution, with the marbles containing an order of magnitude more Cl than the dolomites (2-9 vs. 39-58 ppm, Table 2). Thermal neutron-producing U and Th is only present in rhyolitic tuff samples 5 and 6.

All samples yielded measurable amounts of ^{36}Cl (in carbonates and silicates, Table 2) and ^{10}Be (in quartz, Table 3). ^{36}Cl concentrations range from 28-393×10^3at/g, except for sample 10, which contains a much higher 25×10^6at/g with a 30% analytical uncertainty at 1σ. Because of this high uncertainty and the fact that the ^{36}Cl concentration exceeds the secular equilibrium value, sample 10 is not considered further in this paper.

Similarly, the relatively high U, Th and Cl content of samples 5 and 6 is incompatible with their low ^{36}Cl concentration. Thermal neutrons produced by U and Th are expected to be absorbed by ^{35}Cl to generate excess ^{36}Cl (Alfimov and Ivy-Ochs, 2009). However, no such excess is observed in samples 5 and 6 and so the only way to obtain a finite erosion rate is to assume a physically implausible zero crystallisation age for this rhyolitic material.

On a different note, it is useful to point out that samples 5 and 6 were collected at the same location, at depths of 40 and 110 cm below the surface respectively. Thus, these two samples form a depth profile of sorts. As expected, the ^{36}Cl concentration of the shallow sample exceeds that of the deeper sample (50 vs. 28×10^3at/g, Table 2) with the difference agreeing very well with a simple exponential trend. This, again, appears to be incompatible with the thermal neutron production mechanism, which would exhibit a 'bulge' at shallow depths (Schimmelpfennig et al., 2009). Apart from samples 5, 6 and 10, all other samples are retained for further interpetation.

The exposure history of the Majdanska River Valley is poorly understood. Although the Balkan peninsula is known to have experienced extensive glaciation during the last Ice Age (Menkovic et al., 2004) and the Majdanska River valley bottom is reportedly covered by 'Pleistocene glacial deposits' (Figure 1.b), previous studies have assumed that the ice did not reach the $<$ 1000 m elevations of the Allchar mines (Pavićević et al., 2016). The V-shaped morphology of the Majdanska River valley appears to support the latter scenario (Figure 1.a). Nevertheless, we will quantify the possible effect of glacial erosion by considering two end-member scenarios.

The first scenario assumes that the Allchar area was completely stripped clear by glacial ice, which retreated at 20 ka (= finite exposure scenario). The second scenario assumes an erosion steady-state, in which the field area was never covered by glacial ice. These two scenarios lead to minimum and maximum estimates for the long-term erosion rate, respectively (Table 2 and 3). Three measurements are incompatible with the finite exposure scenario, as they contain too much ^{36}Cl (for sample 7) or ^{10}Be (for samples 11c and 15c). For the remaining samples, the difference in erosion rate between the two scenarios is between 2 and 48%.

6 Discussion

With the exception of sample 10, the ^{36}Cl concentrations are invariably lower than in the Dockhorn et al. (1991) sample, and exhibit an order of magnitude in spacial variability, ranging from 28 to 393×10^3at[^{36}Cl]/g[sample]. This variability is not surprising for bedrock samples, as the assumption of steady-state erosion is only approximately valid at best. Cosmogenic nuclides predominantly form in the upper 1-2 m below the surface and erosion is very variable at this scale.

Three samples contain too much ^{36}Cl (sample 7) or ^{10}Be (samples 11 and 15) to be compatible with a finite exposure history. Taken at face value, these concentrations argue against glacial erosion of the Majdanska River Valley during the last Ice Age and support the hypothesis of steady-state erosion. In order to further investigate the dispersion of the bedrock erosion rates, let us now partition the ^{36}Cl estimates into topographic and lithological categories (Figure 2).

As expected from the sampling strategy outlined in Section 4, samples collected from ridges exhibit the lowest erosion rates, with values ranging from 25 to 112 m/Ma and geometric[1] mean values of 54 and 100 m/Ma for the 20 ka exposure and steady-state erosion histories, respectively. In contrast, the bottom of small canyons hosting minor tributaries of the Majdan River exhibit the highest erosion rates (range: 339-915 m/Ma, means: 559-611 m/Ma).

Samples collected from the slopes between the ridges and the canyon bottoms are characterised by intermediate erosion rates (range: 109-456 m/Ma, means: 208-281 m/Ma). Similarly, catchment-wide erosion rates based on ^{36}Cl in the coarse fraction of modern sediment samples 11, 15 and 20, as well as bedrock sample 19 collected at the bottom of the main river channel also yield intermediate erosion rate estimates

[1]The geometric mean is used because it is the natural average for strictly positive values and is less sensitive to outliers than the arithmetic mean.

(range: 66-648 m/Ma, means: 204-264 m/Ma).

Grouping the bedrock samples according to lithology shows that by far the lowest ^{36}Cl-based erosion rate estimates are observed in the hard andesites of samples 7 and 8 (25-89 m/Ma). At this point it is useful to recall the observation that the calcite marble contains an order of magnitude less natural Cl than the dolomite. This suggests that Cl is lost from dolomite during contact metamorphism. The low ^{35}Cl concentration of the calcite reduces the importance of the thermal neutron production pathway of ^{36}Cl. We would therefore expect the dolomite to contain more cosmogenic ^{36}Cl per gramme of Ca (spallation + thermal neutron absorption) than the calcite (spallation only). This is indeed what is observed, with geometric mean erosion rates of 282-358 m/Ma for the marble and 222-303 m/Ma for the dolomite.

The dispersion of the individual estimate around these mean values (84-864 m/Ma and 109-915 m/Ma, respectively) is admittedly too high to draw any firm conclusions. But what is clear is that the effect of thermal neutrons on the erosion rate estimates is at modest at best, because the difference between the dolomite and the calcite would be much greater if it were not.

As expected, catchment-wide erosion rates based on ^{10}Be-in-quartz are consistently lower than the ^{36}Cl-based estimates (in either bedrock or sediment). This indicates that silicate lithologies erode more slowly than carbonates, a result that is entirely consistent with the ^{36}Cl concentrations in andesite discussed above. Additionally, it is also useful to contemplate the fact that half life of ^{10}Be is more than four times longer than that of ^{36}Cl. This means that ^{10}Be averages erosion rates over longer time scales than ^{36}Cl.

The lower ^{10}Be-based erosion rates could also be taken as evidence for an acceleration of the erosion rates in the Majdanska River Valley over the past million years. Unfortunately, it is impossible to assess the likelihood of this interpretation with the current data.

The ^{36}Cl concentrations in modern river sediments range from 69 to 155×10^3at/g. This dispersion should not surprise us given the small size of the area occupied by carbonate lithologies (13, 11 and 20km^2 for samples 11, 15 and 20, respectively), which may be insufficient to average the upstream heterogeneity in erosion rates. This is made worse by the poor resistence to mechanical abrasion of the carbonate clasts, which biases the detrital carbonate record to nearby sources. Contrastingly, the ^{10}Be concentrations of the fine and the coarse fractions of samples 17 and 20 are remarkably consistent, with four aliquots all containing 67-68$\times10^3$at[^{10}Be]/g[SiO_2].

Samples 11 and 15 contain much more ^{10}Be. There is no satisfactory explanation for these values, although two separate observations cast some doubt on their validity. First, the fact that only one size fraction was analysed for these samples reflects the difficulty in finding sufficient high quality quartz for cosmogenic nuclide analysis in this particular sample. Second, one cannot help but notice that that samples 11 and 15 were collected immediately below the lorandite mining area (Figure 3), which has seen the greatest anthropogenic disturbance. In any case, the striking consistency of the remaining four ^{10}Be erosion rate estimates has led us to accept them as the most representative values for the long-term erosion rate of the Allchar area.

7 Conclusions

This study has re-evaluated the erosion rate of the Majdanska River Valley in southern Macedonia using cosmogenic ^{36}Cl in carbonates from bedrock and modern river sediment, and ^{10}Be in fluvial quartz. Bedrock samples exhibit the greatest range of erosion rate estimates, from 51 to 915 m/Ma, reflecting the small scale variability of erosion rates in both time and space.

The order of magnitude range in erosion rates obtained from our study is not surprising. It is a result of our sampling strategy, which specifically targeted the fastest (canyons) and slowest (ridges) landforms. This

is a very different situation from the study of Pavićević et al. (2016). Their results exhibit a similar degree of dispersion to ours, but for unclear reasons.

In the presence of the observed levels of dispersion, it would be unwise to rely on a single sample of bedrock to determine the erosion rate for the entire Allchar area, as was done by Dockhorn et al. (1991). Samples collected on ridges, in canyons, and in the anthropogenically disturbed Crven Dol and Centralni Deo mining areas are unlikely to yield reliable erosion rates. Carbonate samples collected on slopes and in the Majdan River yield mutually consistent steady-state erosion values of 260-280 m/Ma.

^{10}Be-derived catchment-wide erosion rate estimates for samples 17 and 20 are similarly consistent but significantly lower at 113-125 m/Ma, again assuming an erosional steady-state. These samples were collected upstream and downstream of the lorandite mining area, respectively, and constrain the erosion rate of the quartz-bearing lithologies in the Majdanska River Valley, which occupy roughly twice as much of the draining area as the carbonate lithologies.

The factor of two difference between the carbonate and silicate erosion rates is entirely consistent with the local geology and geomorphology. Closer inspection of the topographic and geologic maps (Figure 1) reveals that the quartz-bearing lithologies (sandstone, gneiss and rhyolite) occupy the higher elevations, whereas the limestones are found in the valleys.

The Pliocene volcanics are currently found on either side of the Majdanska River Valley, at altitudes of more than 850m, where they form a hard protective cap on top of the much softer Triassic carbonates. It is likely that these Pliocene deposits once filled the valley itself, until they were removed by fluvial or fluvioglacial erosion. Once the Majdanska River cut through this hard layer and reached the comparably soft carbonates, erosion would have accelerated to produce the deep valley that is currently observed. Under this scenario, the ^{10}Be-based erosion rates represent the pre-incision values, whereas the ^{36}Cl-based erosion rates represent the current erosion rates of the carbonate areas.

Conservatively extrapolating the ^{10}Be-derived values of 100-120 m/Ma over the 4.3 Ma lifespan of the lorandite deposit at Allchar would suggest the removal of > 450 m of overburden. Adding this amount of shielding to the present 120 m depth of the lorandite deposit would reduce the effect of the muogenic ^{205}Pb contribution sufficiently to be able to see the neutrinogenic component.

Importantly, a recent acceleration of the erosion rate as implied by the ^{36}Cl measurements would further improve the prospects for the lorandite neutrino detector. This is because such an acceleration would mean that the lorandite spent most of its existence at greater depths, only to be exhumed to the surface relatively recently.

Jointly considering the entire body of our twenty-five new erosion rate estimates provides sufficient evidence to discard the single ^{36}Cl measurement of Dockhorn et al. (1991). We would therefore urge the physics community to re-evaluate the feasibility of the lorandite project. Much work remains to be done to make Melvin Freedman's vision a reality (Pavićević et al., 2012). But given the unique advantages of the geological neutrino detector, we would argue that the geological neutrino detector certainly deserves a second chance.

Competing interests

We have no competing interests.

Ethics statement

This work did not involve any living organisms.

Data accessibility

The data are reported in Tables 1, 2 and 3.

Authors' contributions

PV conceived the study, obtained the funding, carried out the field work and wrote the paper, MR carried out the fieldwork and the sample analyses, IS and LB contributed to the sample analyses and the data interpretation, the ASTER team carried out the AMS measurements.

Funding

This research was supported by Leverhulme Grant #RPG-2014-410.

Acknowledgments

PV would like to thank Prof. Günther Korschinek and an anonymous referee for feedback on the submitted manuscript.

References

Alfimov, V. and Ivy-Ochs, S. How well do we understand production of ^{36}Cl in limestone and dolomite? *Quaternary Geochronology*, 4(6):462 – 474, 2009. ISSN 1871-1014. doi: DOI: 10.1016/j.quageo.2009.08.005. Advances in Cosmogenic Isotope Research from CRONUS-EU.

Allen, J. L., Johnson, C. L., Heumann, M. J., Gooley, J., and Gallin, W. New technology and methodology for assessing sandstone composition: A preliminary case study using a quantitative electron microscope scanner (QEMScan). *Geological Society of America Special Papers*, 487:177–194, 2012.

Arnold, M., Merchel, S., Bourlès, D. L., Braucher, R., Benedetti, L., Finkel, R. C., Aumaître, G., Gottdang, A., and Klein, M. The French accelerator mass spectrometry facility ASTER: improved performance and developments. *Nuclear Instruments and Methods in Physics Research Section B: Beam Interactions with Materials and Atoms*, 268(11-12):1954–1959, 2010.

Arnold, M., Aumaître, G., Bourlès, D. L., Keddadouche, K., Braucher, R., Finkel, R. C., Nottoli, E., Benedetti, L., and Merchel, S. The French accelerator mass spectrometry facility ASTER after 4 years: Status and recent developments on ^{36}Cl and ^{129}I. *Nuclear Instruments and Methods in Physics Research Section B: Beam Interactions with Materials and Atoms*, 294:24–28, 2013.

Bahcall, J. N., Calaprice, F., McDonald, A. B., and Totsuka, Y. Solar neutrino experiments: The next generation. *Physics Today*, 49:30–38, 1996. doi: 10.1063/1.881501.

Bierman, P., Gillespie, A., Caffee, M., and Elmore, D. Estimating erosion rates and exposure ages with ^{36}Cl produced by neutron activation. *Geochimica et Cosmochimica Acta*, 59(18):3779–3798, 1995.

Dockhorn, B., Neumaier, S., Hartmann, F. J., Petitjean, C., Faestermann, H., Korschinek, G., Morinaga, H., and Nolte, E. Determination of erosion rates with cosmic ray produced ^{36}Cl. *Zeitschrift fur Physik A Hadrons and Nuclei*, 341:117–119, 1991. doi: 10.1007/BF01281283.

Fink, D., Vogt, S., and Hotchkis, M. Cross-sections for ^{36}Cl from Ti at E_p= 35–150 MeV: applications to in-situ exposure dating. *Nuclear Instruments and Methods in Physics Research Section B: Beam Interactions with Materials and Atoms*, 172(1):861–866, 2000.

Freedman, M. S., Stevens, C. M., Horwitz, E. P., Fuchs, L. H., Lerner, J. L., Goodman, L. S., Childs, W. J., and Hessler, J. Solar neutrinos - Proposal for a new test. *Science*, 193:1117–1119, 1976. doi: 10.1126/science.193.4258.1117.

Jarvis, A., Reuter, H. I., Nelson, A., Guevara, E., et al. Hole-filled SRTM for the globe Version 4. *available from the CGIAR-CSI SRTM 90m Database (http://srtm. csi. cgiar. org)*, 15, 2008.

Menkovic, L., Markovic, M., Cupkovic, T., Pavlovic, R., Trivic, B., and Banjac, N. Glacial morphology of Serbia, with comments on the Pleistocene Glaciation of Monte Negro, Macedonia and Albania. *Developments in Quaternary Sciences*, 2:379–384, 2004.

Merchel, S., Arnold, M., Aumaître, G., Benedetti, L., Bourlès, D., Braucher, R., Alfimov, V., Freeman, S., Steier, P., and Wallner, A. Towards more precise ^{10}Be and ^{36}Cl data from measurements at the 10^{-14} level: Influence of sample preparation. *Nuclear Instruments and Methods in Physics Research Section B: Beam Interactions with Materials and Atoms*, 266(22):4921–4926, 2008.

Neubauer, F., Pavićević, M. K., Genser, J., Jelenković, R., Boev, B., and Amthauer, G. ^{40}Ar/^{39}Ar dating of geological events of the Allchar deposit and its host rocks. *Geochimica et Cosmochimica Acta Supplement*, 73:938, 2009.

Neumaier, S., Nolte, E., and Morinaga, H. Feasibility studies of the geochemical solar neutrino experiment ^{205}Tl(ν,e)^{205}Pb*. *Zeitschrift fur Physik A Hadrons and Nuclei*, 340:415–418, 1991. doi: 10.1007/BF01290330.

Pavićević, M. K. Lorandite from Allchar - A low energy solar neutrino dosimeter. *Nuclear Instruments and Methods in Physics Research A*, 271:287–296, 1988. doi: 10.1016/0168-9002(88)90171-4.

Pavićević, M., Bosch, F., Amthauer, G., Aničin, I., Boev, B., Brüchle, W., Cvetković, V., Djurčić, Z., Henning, W., Jelenković, R., et al. Status and New Data of the Geochemical Determination of the pp-Neutrino Flux by LOREX. *Advances in High Energy Physics*, 2012, 2012.

Pavićević, M., Cvetković, V., Niedermann, S., Pejović, V., Amthauer, G., Boev, B., Bosch, F., Aničin, I., and Henning, W. Erosion rate study at the Allchar deposit (Macedonia) based on radioactive and stable cosmogenic nuclides (^{26}Al, ^{36}Cl, ^{3}He, and ^{21}Ne). *Geochemistry, Geophysics, Geosystems*, 2016.

Schimmelpfennig, I., Benedetti, L., Finkel, R., Pik, R., Blard, P.-H., Bourlès, D., Burnard, P., and Williams, A. Sources of in-situ ^{36}Cl in basaltic rocks. implications for calibration of production rates. *Quaternary Geochronology*, 4(6):441–461, 2009.

Schimmelpfennig, I., Benedetti, L., Garreta, V., Pik, R., Blard, P.-H., Burnard, P., Bourles, D., Finkel, R., Ammon, K., and Dunai, T. Calibration of cosmogenic ^{36}Cl production rates from Ca and K spallation in lava flows from Mt. Etna (38°N, Italy) and Payun Matru (36°S, Argentina). *Geochimica et Cosmochimica Acta*, 75(10):2611–2632, 2011.

Schimmelpfennig, I., Schaefer, J. M., Putnam, A. E., Koffman, T., Benedetti, L., IVY-OCHS, S., Team, A., and Schlüchter, C. 36Cl production rate from K-spallation in the European Alps (Chironico landslide, Switzerland). *Journal of Quaternary Science*, 29(5):407–413, 2014.

Stone, J. O. Air pressure and cosmogenic isotope production. *Journal of Geophysical Research*, 105:23,753–23,759, 2000.

Stone, J., Evans, J., Fifield, L., Allan, G., and Cresswell, R. Cosmogenic chlorine-36 production in calcite by muons. *Geochimica et Cosmochimica Acta*, 62(3):433–454, 1998.

Stone, J. O., Fifield, K., and Vasconcelos, P. Terrestrial Chlorine-36 production from spallation of iron. In *Abstract of 10th International Conference on Accelerator Mass Spectrometry*. Berkeley California, 2005.

Vermeesch, P. CosmoCalc: An Excel add-in for cosmogenic nuclide calculations. *Geochemistry, Geophysics, Geosystems*, 8:8003, 2007. doi: 10.1029/2006GC001530.

von Blanckenburg, F. The control mechanisms of erosion and weathering at basin scale from cosmogenic nuclides in river sediment. *Earth and Planetary Science Letters*, 237:462–479, 2005. doi: 10.1016/j.epsl.2005.06.030.

Figures

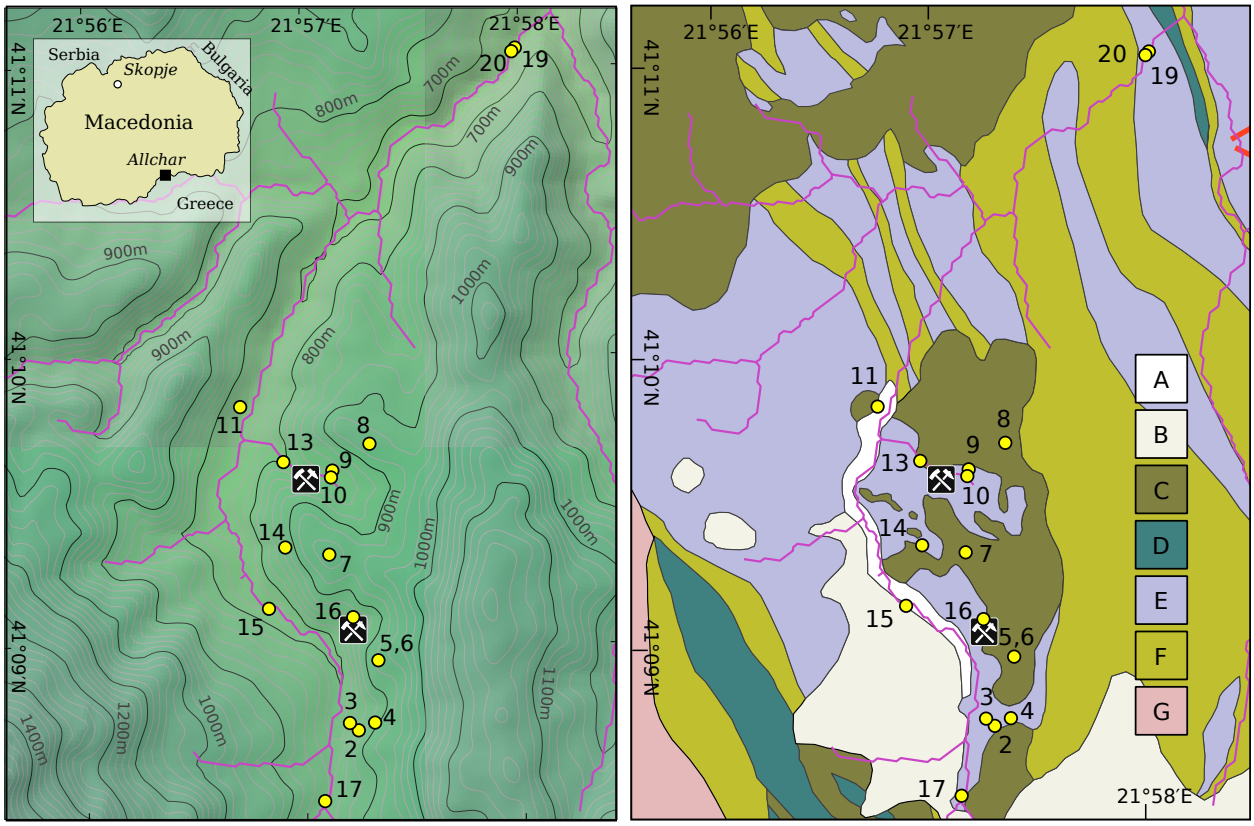

Figure 1: Topographic (left, Jarvis et al., 2008) and geologic map (right) of the Allchar area with indication of the Crven Dol (North) and Centralni Deo (South) mine locations, and the sample locations (yellow circles). A – modern alluvium, B – Quaternary sediments, including (fluvio-)glacial deposits, C – Pliocene andesites, rhyolites and tuffs, D – Jurassic serpentinites, E – Triassic limestones and dolomites, F – Mesozoic sandstones and slates, G – Precambrian gneiss.

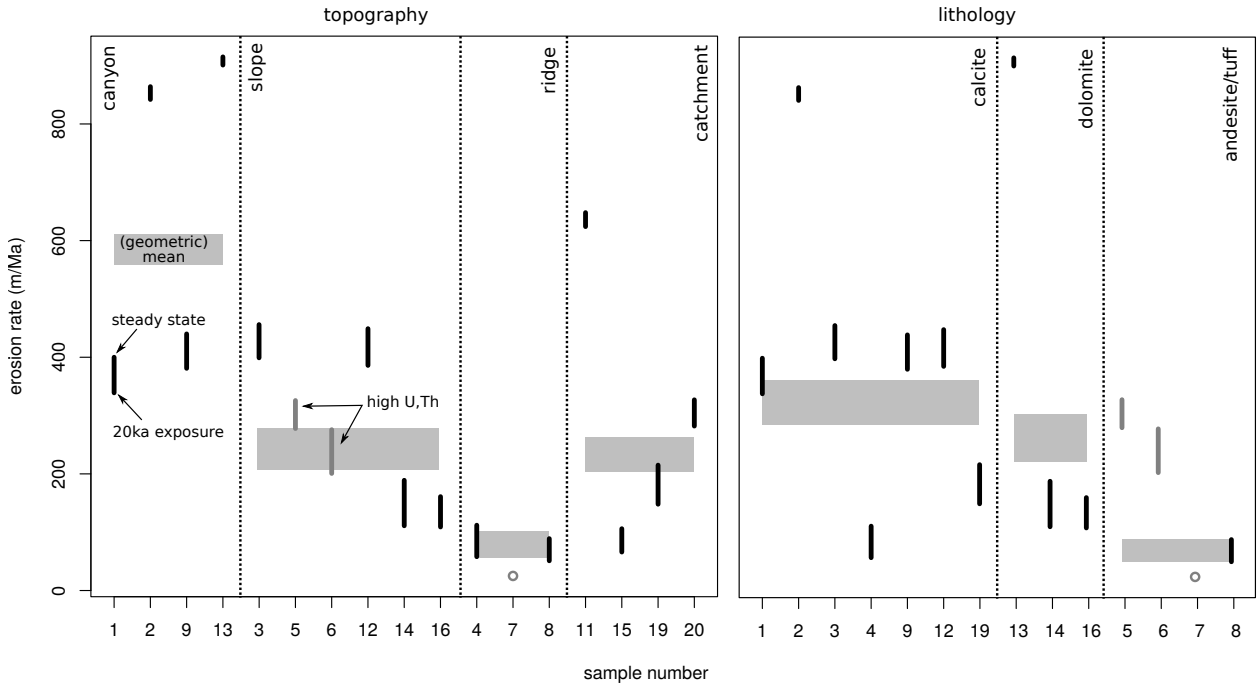

Figure 2: ^{36}Cl-based apparent erosion rates for the Allchar area grouped according to topographic location (left) and lithology (right). Vertical bars connect the erosion rate estimates assuming steady-state (top) and a 20 ka exposure history (bottom), respectively. Similarly, the geometric mean erosion rates are shown as boxes whose top and bottom margins correspond to the steady-state and finite exposure scenarios. Samples 5 and 6 contain high concentrations of thermal neutron-producing U and Th for which an erosion rate can only be calculated under the assumption of an unrealistic zero crystallisation age. Sample 7 contains too much ^{36}Cl to be compatible with the 20 ka exposure scenario.

Tables

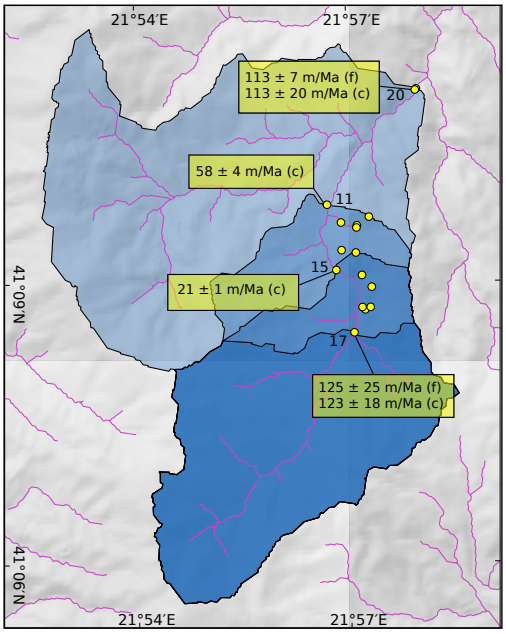

Figure 3: Catchment area of the Majdan River and its tributaries upstream of the four modern sediment samples, with indication of the ^{10}Be-based catchment-wide erosion rate estimates. (c) refers to the coarse and (f) to the fine fraction.

sample	location	lithology	ρ [g/cm^3]	lat	lon	elevation [m]	d [cm]	t [cm]	S_t
1	canyon	marble	1.70	41.1453	21.9565	913	0	4	0.968
2	canyon	marble	2.70	41.1451	21.954	870	0	6	0.952
3	slope	marble	2.70	41.1455	21.9533	844	0	5	0.960
4	ridge	marble	2.68	41.1455	21.9552	908	0	6	0.952
5	slope	tuff	1.86	41.1491	21.9555	940	40	10	0.922
6	slope	tuff	1.87	41.1491	21.9555	940	110	10	0.922
7	ridge	andesite	2.56	41.1552	21.9519	962	0	1	0.992
8	ridge	andesite	2.41	41.1616	21.9550	959	0	1	0.992
9	canyon	marble	2.70	41.1600	21.9522	831	0	5	0.960
10	slope	marble	-	41.1597	21.9521	837	0	7	0.944
11	sediment	sand/gravel	2.80	41.1638	21.9452	721/1151/1323	-	-	-
12	slope	marble	2.59	41.1643	21.9497	817	0	7.5	0.940
13	slope	dolomite	2.80	41.1606	21.9484	787	0	3	0.976
14	slope	dolomite	2.68	41.1556	21.9485	889	10	10	0.922
15	sediment	sand/gravel	-	41.1521	21.9472	779/1205/1347	-	-	-
16	slope	dolomite	2.76	41.1512	21.9532	847	0	10	0.922
17	sediment	sand/gravel	-	41.1410	21.9513	833/1249/1387	-	-	-
19	thalweg	marble	2.69	41.1843	21.9664	620	0	1	0.992
20	sediment	sand/gravel	-	41.1841	21.9662	614/1055/1259	-	-	-

Table 1: Sample locations. ρ is rock density, d sampling depth, t sample thickness, and S_t the topographic shielding factor (Vermeesch, 2007). Three elevations are given for the modern sediment samples, written as $x/y/z$ where x is the elevation of the sample location, y the average elevation of the upstream catchment area that is occupied by carbonates, and z the average elevation of the quartz-bearing parts of the catchment area.

sample #	CaO [wt%]	K_2O [wt%]	Fe_2O_3 [wt%]	Cl [ppm]	Th [ppm]	U [ppm]	^{36}Cl [×1000 at/g]	$\epsilon(20\ ka)$ [m/Ma]	$\epsilon(\infty)$ [m/Ma]
1	52	0	0	4.9	0	0	94(5)	339(17)	400(20)
2	54	0	0	4.8	0	0	41(3)	842(61)	864(62)
3	54	0	0	2.2	0	0	86(5)	399(28)	456(27)
4	56	0	0	2.0	0	0	361(12)	58(2)	112(4)
5	0.6	6.6	1.5	33	56	12	50(5)	276(35)*	324(41)*
6	0.5	6.4	0.9	16	56	12	28(3)	199(37)*	274(51)*
7	8.8	1.3	0.6	7.9	0	0	393(23)	-	25.0(2)
8	5.6	2.1	0	2.5	0	0	106(7)	51(4)	89(7)
9	56	0	0	2.7	0	0	85(4)	381(19)	440(22)
10	55	0	0	8.3	0	0	25322(7579)	-	-
11c	23	0	0	69	0	0	69(4)	624(39)	648(40)
12	56	0	0	0.7	0	0	84(4)	386(21)	449(25)
13	33	0	0	57	0	0	36(3)	901(87)	915(89)
14	32	0	0	48	0	1	232(11)	111(5)	189(9)
15c	15	0	0	39	0	0	155(7)	66(3)	106(6)
16	31	0	0	39	0	0	185(8)	109(5)	161(7)
19	56	0	0	8.9	0	0	169(6)	148(6)	215(8)
20c	21	0	0	69	0	0	109(5)	282(13)	327(15)

Table 2: Cosmogenic ^{36}Cl results. $\epsilon(20\ ka)$ and $\epsilon(\infty)$ represent the erosion rate estimates assuming a 20 ka exposure history and erosional steady-state, respectively. 11c, 15c and 20c refer to the coarse fraction of samples 11, 15 and 20. Erosion rates for samples 5 and 6 (marked by $*$) assume a(n unrealistic) zero crystallisation age and are not considered further. Chemical compositions refer to the solid (silicates) and liquid (carbonates) splits taken after etching. Bulk compositions of the silicate rocks prior to etching are provided in the Online Supplement.

sample #	^{10}Be [×1000 at/g]	$\epsilon(20\ ka)$ [m/Ma]	$\epsilon(\infty)$ [m/Ma]
11c	136(9)	-	58(4)
15c	371(16)	-	21(1)
17f	67(13)	114(22)	125(25)
17c	68(10)	112(16)	123(18)
20f	68(4)	101(6)	113(7)
20c	67(12)	101(18)	113(20)

Table 3: Cosmogenic ^{10}Be results. 17f and 20f correspond to the fine fractions of samples 17 and 20, respectively. The high ^{10}Be concentrations of samples 11 and 15 are incompatible with a 20 ka erosion history.